

Dissipative residual layers for unsupervised implicit parameterization of data manifolds

1st Viktor Reshniak

Data Analysis and Machine Learning Group

Oak Ridge National Laboratory

Oak Ridge, TN 37831

reshniakv@ornl.gov

<https://orcid.org/0000-0003-1545-4462>

Abstract—We propose an unsupervised technique for implicit parameterization of data manifolds. In our approach, the data is assumed belonging to a lower dimensional manifold in a higher dimensional space, and the data points are viewed as the endpoints of the trajectories originating outside the manifold. Under this assumption, the data manifold is an attractive manifold of a dynamical system to be estimated. We parameterize such dynamical system with a residual neural network and propose a spectral localization technique to ensure it is locally attractive in the vicinity of data. We also present initialization and additional regularization of the proposed residual layers. We mention the importance of the considered problem for the tasks of reinforcement learning and support our discussion with examples demonstrating the performance of the proposed layers in denoising and generative tasks.

Index Terms—residual network, attractive manifold, spectral localization, stability

I. INTRODUCTION

Overparameterization has proven to be a blessing rather than a curse of modern neural network architectures. It is essential for finding nearly-global optimal solutions by reducing the number of spurious local minima [16], [1], [14], and has been proven to be necessary for learning models that are both robust and accurate [4], [5]. Empirical observations support these result by demonstrating that high capacity is required to defend against strong adversaries in practice [13].

Of course, overparameterization itself is not sufficient to guarantee stable and predictable behavior of trained models. Careless application of deep networks to out-of-distribution and unforeseen data can easily lead to catastrophic behavior hindering their use in safety critical tasks. For example, in reinforcement learning, the ability of models to safely recover from exploratory behavior and random perturbations is required to learn stable optimal policies [11], [3]. It would be beneficial if one has a non-intrusive approach that can be easily added to an existing architecture and improve the stability of a model without altering its behavior on the observed experimental data. Here we make a small step towards this goal and propose an end-to-end-trainable layer for the implicit parameterization of data as a stable manifold of a dynamical system. The parameter estimation in this case is given by the optimal control

problem [8]

$$\min_{\gamma_t} \mathbb{E}_{\mu} \left[L(y_T, f(x)) + \int_0^T R(\gamma_t, y_t) dt \right], \quad (1)$$

$$\text{subject to } y_t = F(\gamma_t, x), \quad (2)$$

where $L(y_T, f(x))$ is a terminal loss function, $R(\gamma_t, y_t)$ is a regularizer, μ is a probability distribution of the input-target data pairs $(x, f(x))$, and the evolution of y_t in phase space is driven by a flow $F : \mathbb{R}^p \times \mathbb{R}^d \rightarrow \mathbb{R}^d$ through the input data $y_0 = x \in \mathbb{R}^d$. Typical examples include residual layers [10] or neural ODEs [6], i.e.,

$$y_t = y_{t-1} + F(\gamma_t, y_{t-1}) \quad \text{and} \quad \dot{y}_t = F(\gamma_t, y_{t-1}),$$

and their various extensions.

Overparameterization benefits dynamical system reformulation of neural networks as well. Dupont et al. [7] showed that Neural ODEs preserve the topology of the input space implying that certain functions cannot be represented by continuous flows. Augmenting the original space with additional dimensions allowed to resolve this issue and lead to models that generalized better and produced simpler flows with a lower computational cost. In fact, many DNNs can be viewed as dynamical systems embedded in a higher dimensional space. For example, the number of pixels in images commonly exceeds the dimension of the corresponding image manifolds facilitating efficient out-of-manifold adversarial attacks [12].

Robust/adversarial training with data augmentation reduces standard accuracy and generalizes poorly to unforeseen data perturbations [18], [17]. In this effort, we propose an unsupervised technique for implicit parameterization of data manifolds that does not require explicit data augmentation. In our approach, the data is assumed belonging to a lower dimensional manifold in a higher dimensional space, and the data points are viewed as the endpoints of the trajectories originating outside the manifold. Under this assumption, the data manifold is an attractive manifold of a dynamical system to be estimated. For the representation of such dynamical system, we introduce dissipative residual layers with explicit Lipschitz constants and a spectral localization approach that allows for the precise control of the spectrum of such layers. The proposed layer is end-to-end trainable and can be easily added into existing

network architectures.

II. DISSIPATIVE RESIDUAL LAYERS

A. Definitions

Following the definition proposed in [15], consider the trajectory generated by the implicit residual layer

$$y = x + F(\gamma, (1 - \theta)x + \theta y). \quad (3)$$

and another perturbed trajectory given by

$$\bar{y} = \bar{x} + F(\gamma, (1 - \theta)\bar{x} + \theta\bar{y}).$$

By linearizing $F(\gamma, \cdot)$ around the reference trajectory, the evolution of the perturbation $\bar{y} - y$ is described by the linear system

$$\begin{aligned} \bar{y} - y &= \left(I - \theta \frac{\partial F(\gamma, z)}{\partial z} \right)^{-1} \left(I + (1 - \theta) \frac{\partial F(\gamma, z)}{\partial z} \right) (\bar{x} - x) \\ &= \mathcal{R}_\theta \left(\frac{\partial F(\gamma, z)}{\partial z} \right) (\bar{x} - x), \quad z = (1 - \theta)x + \theta y. \end{aligned}$$

The eigenvalues of the Jacobian $D_z F(\gamma, z)$ determine the local stability properties of the system in (3). This can be seen by looking at the Jordan normal form J of $D_z F(\gamma, z) = PJP^{-1}$ such that

$$\mathcal{R}_\theta \left(\frac{\partial F(\gamma, z)}{\partial z} \right) = \mathcal{R}_\theta (PJP^{-1}) = P\mathcal{R}_\theta(J)P^{-1}.$$

The diagonal of the matrix J contains the eigenvalues of the Jacobian $D_z F(\gamma, z)$, and the diagonal of the matrix $\mathcal{R}_\theta(J)$ is obtained by evaluating the matrix function \mathcal{R}_θ elementwise on the diagonal entries of J . In the numerical analysis of ordinary differential equations, e.g. [9], the corresponding scalar function \mathcal{R}_θ is known as the **stability function** of (3). It is hence given by

$$\mathcal{R}_\theta(z) = \frac{1 + (1 - \theta)z}{1 - \theta z}, \quad z \in \mathbb{C} \quad (4)$$

and describes the evolution of the eigenmodes of the linear perturbation to the solution of (3), i.e.,

$$\bar{x} - x \in \text{span}(v_1, \dots, v_d)$$

implies

$$\bar{y} - y \in \text{span}(\mathcal{R}_\theta(\lambda_1)v_1, \dots, \mathcal{R}_\theta(\lambda_d)v_d),$$

where λ_i, v_i are the eigenvalues and (generalized) eigenvectors of the Jacobian $D_z F(\gamma, z)$.

Definition 1. Stability region is a set of all $z \in \mathbb{C}$ such that $|\mathcal{R}_\theta(z)| < 1$. It contains those eigenvalues of the Jacobian $D_z F(\gamma, z)$ corresponding to stable subspaces of the linearized system. Perturbations along such stable directions asymptotically vanish.

Definition 2. If all eigenvalues of the Jacobian evaluated at any arbitrary point are within the stability region of a layer, then it is unconditionally stable and we call it a **dissipative residual layer**.

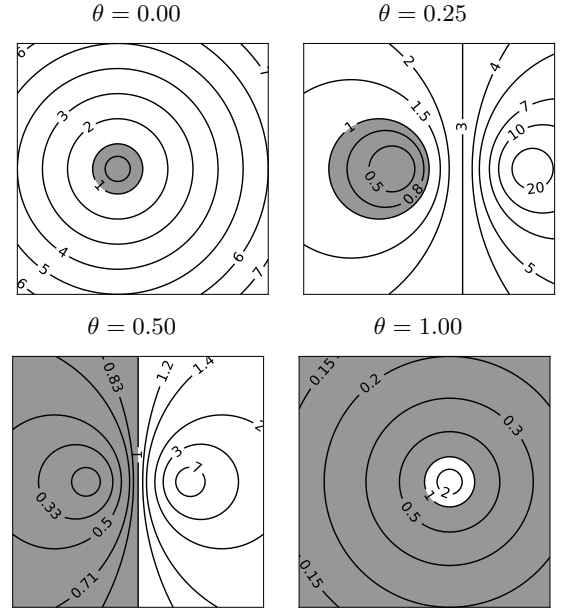


Fig. 1. Stability regions (grey) and contours of $|\mathcal{R}_\theta(z)|$.

Figure 1 illustrates stability regions of several implicit residual layers.

B. Spectral normalization and localization

We assume that the vector field $F(\gamma, x)$ is a composition of affine maps and element-wise activations, i.e.,

$$F(\gamma, x) = \phi_n \circ \phi_{n-1} \circ \dots \circ \phi_1 \circ x$$

with

$$\phi_i \circ x = \sigma(\gamma_i \circ x + b_i).$$

The Lipschitz constant of $F(\gamma, x)$ is given by

$$\text{Lip}(F) := \sup_x \left\| \frac{\partial F(\gamma, x)}{\partial x} \right\| \leq |\sigma|^n \prod_{i=1}^n \|\gamma_i\|,$$

where $|\sigma| := \sup_x |\sigma'(x)|$ and $\|\cdot\|$ is the spectral norm. Hence by setting

$$\tilde{\gamma}_i = \frac{\gamma_i}{|\sigma| \cdot \|\gamma_i\|},$$

we get $\text{Lip}(F) \leq 1$ **uniformly in x** . Note that for many standard activation functions, including ReLU, hyperbolic tangent, and sigmoid, $|\sigma| = 1$.

From the definition of spectral radius, we have

$$\rho \left(\frac{\partial F(\tilde{\gamma}, x)}{\partial x} \right) \leq \left\| \frac{\partial F(\tilde{\gamma}, x)}{\partial x} \right\| \leq 1 \quad \rightarrow \quad \lambda_i \in \mathcal{B}(0, 1) \quad \forall i,$$

and thus all eigenvalues of $D_x F(\tilde{\gamma}, x)$ are located in the unit circle $\mathcal{B}(0, 1) \in \mathbb{C}$. By denoting $\tilde{F}(\gamma, x) := F(\tilde{\gamma}, x)$ and by appropriately scaling and shifting $\tilde{F}(\gamma, x)$, we redefine the vector field as

$$F(\gamma, x) := c \cdot x + r \cdot \tilde{F}(\gamma, x) \quad \rightarrow \quad \lambda_i \in \mathcal{B}(c, r) \quad \forall i,$$

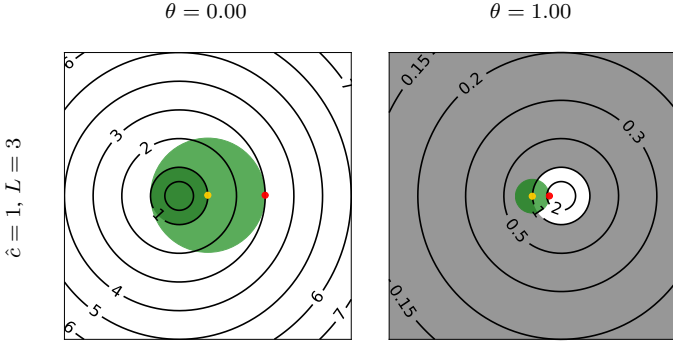


Fig. 2. Contours of $|\mathcal{R}_\theta|$ with disks $\mathcal{B}(\mathcal{R}_\theta^{-1}(\hat{c}), \mathcal{R}_\theta^{-1}(L) - \mathcal{R}_\theta^{-1}(\hat{c}))$; yellow and red points correspond to $\mathcal{R}_\theta^{-1}(\hat{c})$ and $\mathcal{R}_\theta^{-1}(L)$ respectively. Note that $\sup_{\lambda \in \mathcal{B}} |\mathcal{R}_\theta(\lambda)| = |\mathcal{R}_\theta(\bullet)| = L$.

so that all eigenvalues of $D_x F(\gamma, x)$ are now located in the disc $\mathcal{B}(c, r)$ with radius r centered at c .

It is convenient to define the disk $\mathcal{B}(c, r)$ in terms of the values of the stability function \mathcal{R}_θ as follows

$$c := \mathcal{R}_\theta^{-1}(\hat{c}), \quad r := \max\left(0, \mathcal{R}_\theta^{-1}(L) - c\right)$$

with

$$\hat{c}(\gamma_c) := \hat{c}_1 + S(\gamma_c) \cdot (\hat{c}_2 - \hat{c}_1), \quad \hat{c}_i > 0, \quad (5)$$

$$L(\gamma_L) := L_1 + S(\gamma_L) \cdot (L_2 - L_1), \quad L_i > 0 \quad (6)$$

where $S(\cdot)$ is the sigmoid function, γ_c, γ_L are the scalar valued parameters and \mathcal{R}_θ^{-1} is the inverse stability function

$$\mathcal{R}_\theta(z) = \frac{1 + (1 - \theta)z}{1 - \theta z} \rightarrow \mathcal{R}_\theta^{-1}(z) = \frac{1 - z}{\theta(1 - z) - 1}.$$

It can be shown that for $c > \mathcal{R}_\theta^{-1}(0)$ and $\lambda \in \mathcal{B}(c, r)$, $\mathcal{R}_\theta(\lambda)$ attains its maximum value at λ with largest $\text{Re}(\lambda)$, see Figure 2 for illustration. This value defines the Lipschitz constant of a residual layer in (3) as follows

$$\sup_{\lambda \in \mathcal{B}(c, r)} |\mathcal{R}_\theta(\lambda)| = \max(\hat{c}(\gamma_c), L(\gamma_L)).$$

The above expression allows to explicitly bound the Lipschitz constant within the given range by means of \hat{c}_i, L_i in (5)-(6) and also to include it into the optimization problem through learnable parameters γ_c, γ_L .

Theorem 1. *The residual layer is dissipative if its vector field is parameterized as*

$$F(\gamma, x) := c \cdot x + r \cdot \tilde{F}(\gamma, x)$$

with

$$c := \mathcal{R}_\theta^{-1}(1 - S(\gamma_c)), \\ r := \max\left(0, \mathcal{R}_\theta^{-1}(1 - S(\gamma_L)) - c\right).$$

Proof. Follows directly from Definition 2 since both $\hat{c}, L \in (0, 1)$. \square

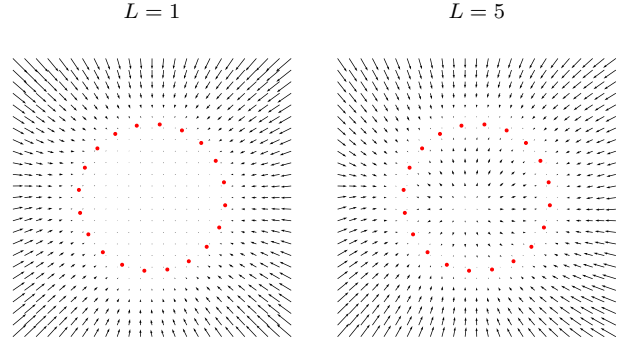


Fig. 3. Vector fields of a residual layer trained with different bounds on the Lipschitz constant.

Remark. Dissipative layers have the obvious benefit of being unconditionally stable uniformly for all inputs. However, Figure 3 shows the situation when the dissipativity condition becomes overly restrictive. The vector fields in this example were trained to vanish on the boundary of the circle while being locally attractive to it. According to the Gauss's theorem, the total of the sources in the closed volume is equal to the flux of the vector field across the boundary. Since the vector field vanishes on the boundary, it must have sources inside the volume to satisfy the condition of local attractiveness. To get nontrivial solutions, we are forced to allow for the Lipschitz constant of the layer to be greater than one to include the region of positive divergence. In all examples below, we will use $L \in [1, 5]$.

C. Dissipative manifolds

Definition 3. *We define the **dissipative manifold** \mathcal{M}_d as a set of points that has vanishing vector field and is locally attractive. In other words, it is the level set*

$$\mathcal{M}_d = \{x : \|F(\gamma, x)\|^2 = 0, |\mathcal{R}_\theta(\lambda_i)| < 1\}$$

for all eigenvalues λ_i of the Jacobian $D_x F(\gamma, x)$, $x \in \mathcal{M}_d$.

According to the above definition, any point on the manifold must be stationary, and any point close enough to the manifold should be transported back to the manifold by the flow of the corresponding residual layer.

The first goal can be achieved by regularizing the magnitude of the vector field

$$R_F(\gamma) := \|F(\gamma, x)\|^2. \quad (7)$$

To achieve the second goal, for every data point on the manifold, we are interested in concentrating as many eigenvalues of the corresponding Jacobian as possible in the vicinity of $\mathcal{R}_\theta^{-1}(0)$ so that the corresponding degrees of freedom effectively vanish. For this purpose, use the following bound

$$\sum_i \left| \lambda_i(\mathcal{R}_\theta(D_x F)) \right|^2 \leq \sum_i \sigma_i^2(\mathcal{R}_\theta(D_x F)) \\ = \|\mathcal{R}_\theta(D_x F)\|_F^2 = \text{Tr}(\mathcal{R}_\theta(D_x F)^T \mathcal{R}_\theta(D_x F))$$

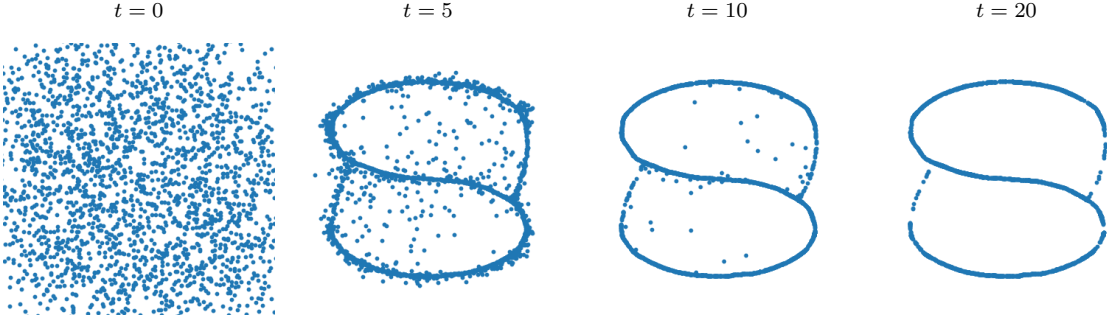


Fig. 4. One-dimensional dissipative manifold in two-dimensional space.

and consider the trace regularization of the form

$$R_\lambda(\gamma) := \text{Tr} \left(\mathcal{R}_\theta(D_x F)^T \mathcal{R}_\theta(D_x F) \right). \quad (8)$$

The Frobenius norm of the Jacobian can be efficiently estimated using the stochastic Hutchinson estimator, see [15] for an example.

Regularizers in (7)-(8) are local to the data manifold since they only require original data points. Better results can be obtained by considering nonlocal perturbations in the directions orthogonal to the manifold. These orthogonal directions can be obtained trivially by computing the gradient of the level set at each point as $n = \nabla \|F(\gamma, x + \epsilon)\|^2$. The small random perturbation ϵ is chosen to ensure the uniqueness of the gradient. The corresponding regularization for the explicit residual layer is then given by

$$R_n(\gamma) = \|F(\gamma, x + \alpha n) + \alpha n\|^2 \quad (9)$$

for some small $\alpha > 0$. More perturbation points can be obtained by stepping backwards in time along the trajectory ending at $x + \alpha n$. This gives

$$R_{adj}(\gamma) = \sum_j \|F(\gamma, x_j) + x_j - x\|^2, \quad (10)$$

where x_j is the trajectory generated by the adjoint solver, e.g.,

$$y = x + F(x) \quad \rightarrow \quad x = y - F(x).$$

Figure 5 illustrates the impact of the number of steps in (10) on the learned dynamics. Adding more steps in (10) favors more aggressive exploration of the space around the manifold. One can see from the Figure that this can result in a better adaptation to the geometry of the data. Figure 4 also shows the learned evolution of the random point cloud that is attracted to the original data manifold.

III. EXAMPLE

As a final example demonstrating the properties of the proposed manifold representation approach, consider the digits dataset from UCI ML Repository [2]. This dataset contains 5620 8x8 pixel 16 bit images of handwritten digits each treated as a vector of size 64.

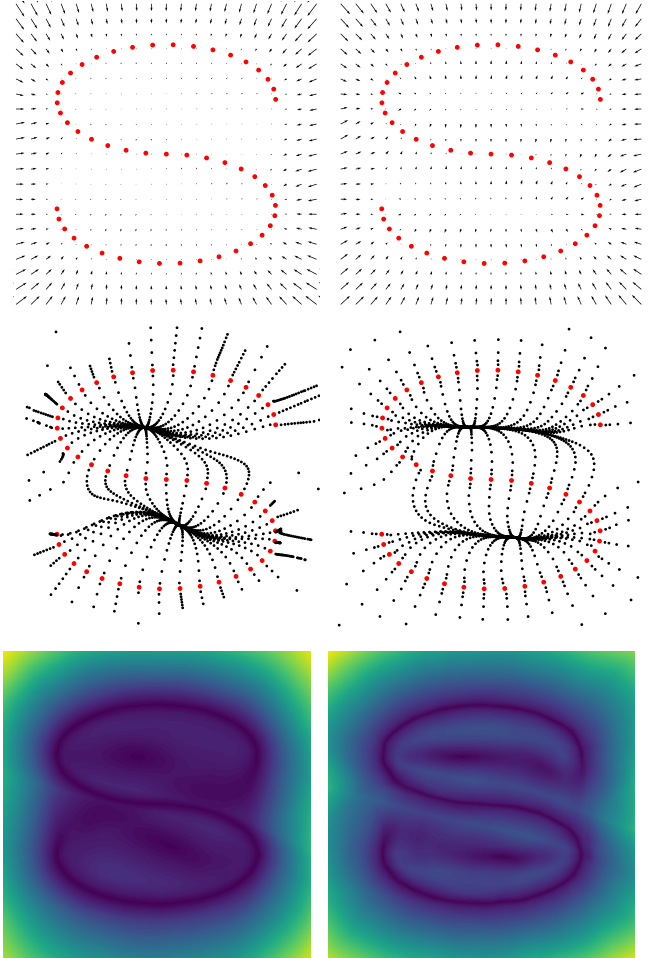


Fig. 5. Vector fields, adjoint trajectories, and the level sets of the 2d curve for 1 (left) and 3 (right) steps of the adjoint solver in regularizer (10).

We parameterized the vector field of the residual layer by a ReLU network of depth 2 and width 1000. We trained the explicit ($\theta = 0$) residual layer by minimizing the regularizers in (7) and (8) using Adam optimizer with step size 10^{-3} for 10000 epochs.

Figures 6 and 7 show the outcome of the trained layer for the inputs corrupted with additive and truncated Gaussian noise.

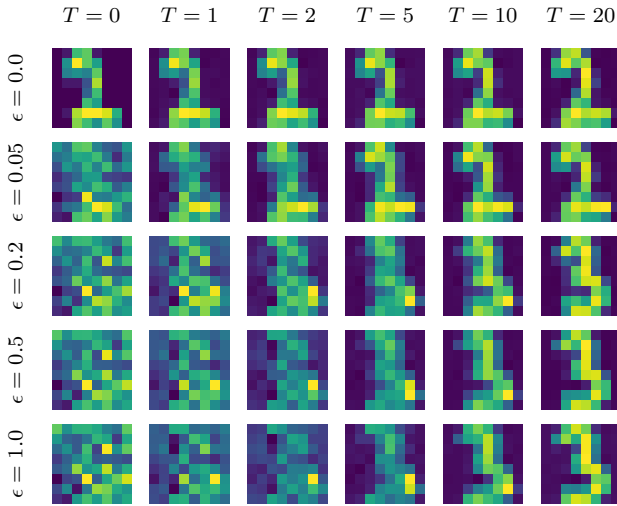


Fig. 6. Denoising of a digit corrupted with additive Gaussian noise.

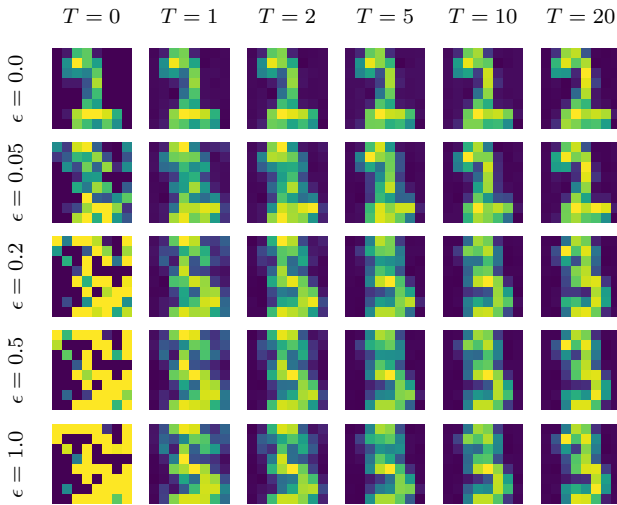


Fig. 7. Denoising of a digit corrupted with truncated Gaussian noise.

One can see that for the noise with variance $\epsilon = 0.05$, the layer was able to reproduce the original image very accurately even though the corrupted image is difficult to recognize visually. For the larger levels of noise, the layer did not reproduce the original image but still produced a very clear output of a different digit. This indicates that the learned vector field performs projection on the original data manifold as desired. Figure 8 supports this finding by illustrating the completion of partially missing data. It shows that the proposed data manifold representation approach can be also used for generative tasks.

IV. CONCLUSIONS AND FUTURE WORK

A method to construct an implicit parameterization of data manifolds was proposed. It is end-to-end trainable and can be easily added to any existing network. Performance of the method was demonstrated on denoising and generative tasks. The obtained results are encouraging but more efforts are required for the detailed comparison with existing alternatives. Potential applications include those that can benefit from

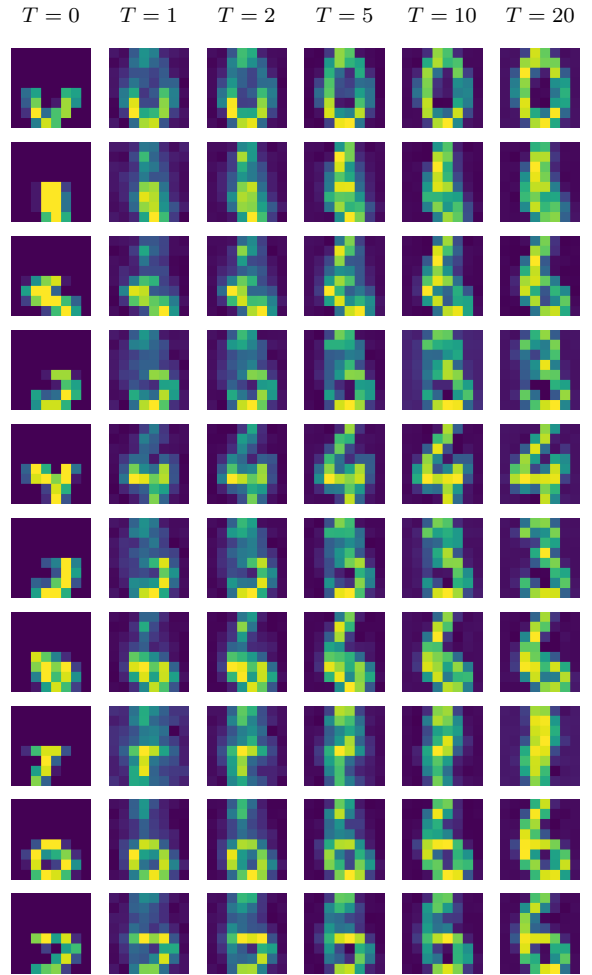


Fig. 8. Generating digits from missing data

stabilizing their latent dynamics. The problem of stabilizing optimal policies in the tasks of reinforcement learning is of particular interest and will be studied in future works.

REFERENCES

- [1] Zeyuan Allen-Zhu, Yuanzhi Li, and Zhao Song. A convergence theory for deep learning via over-parameterization. In Kamalika Chaudhuri and Ruslan Salakhutdinov, editors, *Proceedings of the 36th International Conference on Machine Learning*, volume 97 of *Proceedings of Machine Learning Research*, pages 242–252. PMLR, 09–15 Jun 2019.
- [2] E Alpaydin and C Kaynak. Optical recognition of handwritten digits data set. *UCI Machine Learning Repository*, 1998.
- [3] Felix Berkenkamp, Matteo Turchetta, Angela Schoellig, and Andreas Krause. Safe model-based reinforcement learning with stability guarantees. *Advances in neural information processing systems*, 30, 2017.
- [4] Sebastien Bubeck, Yuanzhi Li, and Dheeraj Nagaraj. A law of robustness for two-layers neural networks. *Computing Research Repository (CoRR)*, September 2020.
- [5] Sebastien Bubeck and Mark Sellke. A universal law of robustness via isoperimetry. In A. Beygelzimer, Y. Dauphin, P. Liang, and J. Wortman Vaughan, editors, *Advances in Neural Information Processing Systems*, 2021.
- [6] Tian Qi Chen, Yulia Rubanova, Jesse Bettencourt, and David K Duvenaud. Neural ordinary differential equations. In S. Bengio, H. Wallach, H. Larochelle, K. Grauman, N. Cesa-Bianchi, and R. Garnett, editors, *Advances in Neural Information Processing Systems 31*, pages 6571–6583. Curran Associates, Inc., 2018.

- [7] Emilien Dupont, Arnaud Doucet, and Yee Whye Teh. Augmented Neural ODEs. In H. Wallach, H. Larochelle, A. Beygelzimer, F. d'Alché-Buc, E. Fox, and R. Garnett, editors, *Advances in Neural Information Processing Systems*, volume 32. Curran Associates, Inc., 2019.
- [8] Weinan E, Jiequn Han, and Qianxiao Li. A mean-field optimal control formulation of deep learning. *Research in the Mathematical Sciences*, 6(10), 2019.
- [9] Ernst Hairer, Syvert P. Nørsett, and Gerhard Wanner. *Solving Ordinary Differential Equations I, Nonstiff Problems*, volume 8 of *Springer Series in Computational Mathematics*. Springer-Verlag Berlin Heidelberg, 1993.
- [10] Kaiming He, Xiangyu Zhang, Shaoqing Ren, and Jian Sun. Identity mappings in deep residual networks. In Bastian Leibe, Jiri Matas, Nicu Sebe, and Max Welling, editors, *Computer Vision – ECCV 2016*, pages 630–645. Cham, 2016. Springer International Publishing.
- [11] Hassan K Khalil. *Nonlinear control*, volume 406. Pearson New York, 2015.
- [12] Wei-An Lin, Chun Pong Lau, Alexander Levine, Rama Chellappa, and Soheil Feizi. Dual Manifold Adversarial Robustness: Defense against Lp and non-Lp Adversarial Attacks. *arXiv preprint arXiv:2009.02470*, 2020.
- [13] Aleksander Madry, Aleksandar Makelov, Ludwig Schmidt, Dimitris Tsipras, and Adrian Vladu. Towards deep learning models resistant to adversarial attacks. In *International Conference on Learning Representations*, 2018.
- [14] Samet Oymak and Mahdi Soltanolkotabi. Overparameterized nonlinear learning: Gradient descent takes the shortest path? In Kamalika Chaudhuri and Ruslan Salakhutdinov, editors, *Proceedings of the 36th International Conference on Machine Learning*, volume 97 of *Proceedings of Machine Learning Research*, pages 4951–4960. PMLR, 09–15 Jun 2019.
- [15] Viktor Reshniak and Clayton G. Webster. Robust learning with implicit residual networks. *Machine Learning and Knowledge Extraction*, 3(1):34–55, 2021.
- [16] Itay Safran and Ohad Shamir. Spurious local minima are common in two-layer ReLU neural networks. In Jennifer Dy and Andreas Krause, editors, *Proceedings of the 35th International Conference on Machine Learning*, volume 80 of *Proceedings of Machine Learning Research*, pages 4433–4441. PMLR, 10–15 Jul 2018.
- [17] Yang Song, Rui Shu, Nate Kushman, and Stefano Ermon. Constructing unrestricted adversarial examples with generative models. In S. Bengio, H. Wallach, H. Larochelle, K. Grauman, N. Cesa-Bianchi, and R. Garnett, editors, *Advances in Neural Information Processing Systems*, volume 31. Curran Associates, Inc., 2018.
- [18] Dimitris Tsipras, Shibani Santurkar, Logan Engstrom, Alexander Turner, and Aleksander Madry. Robustness may be at odds with accuracy. In *International Conference on Learning Representations*, 2019.